

WEIGHTED GUIDED IMAGE FILTER USING MONOGENIC PHASE CONGRUENCY

JUNRUI LV, SHIFENG QI AND XUEGANG LUO

School of Mathematics and Computer Science
Panzhuhua University
No. 10, Airport Road, Eastern District, Panzhuhua 617000, P. R. China
21658388@qq.com

Received May 2016; accepted August 2016

ABSTRACT. *The original guided image filter is not robust enough because it occupies the same local linear model among all the local patches while ignoring the texture difference. Weighted guided image filter (WGIF) is introduced by incorporating a monogenic phase congruency weighting for edge-awareness into an existing guided image filter (GIF) to avoid halo artifacts for image denoising. The fixed regularization parameter of GIF cannot adapt to the grey scale difference between flat and edge patches. Therefore, traditional GIF cannot represent the image well near some edges. From the perspective of visual perception, monogenic phase congruency, which has definite immunity to noise, can describe preferably the information of edge and texture. It is used to penalize the fixed regularization parameter to adapt to edge-aware weighting constraints. Compared with traditional GIF for image denoising and other state-of-the-art methods with SSIM and PSNR as image quality metric, experimental results showed the proposed denoising algorithm can not only remove noise efficiently and reduce halo artifacts, but also preserve the edge texture well.*

Keywords: Image denoising, Monogenic phase congruency, Weighted guided image filter

1. Introduction. Image denoising is one of the important tasks for various applications in image processing. Noise reduction and edge-preserving are two main performance metrics of image denoising algorithms. Many algorithms [1-3] have been developed to recover image missing information in the process of collection, processing, compression, storage, and transmission. However, it is still a challenging problem that achieves simultaneously both metrics.

Recently, a newer filter called the guided image filter (GIF) was proposed in [4]. GIF is an edge-preserving smoothing algorithm for sharpening and denoising simultaneously. Due to superior performance of GIF, it has been applied to the fields of computational photography and image processing. Typical examples include image sharpening [5], image fusion [6], single image haze removal [7], etc. Unfortunately, it is possible to be absent of the structure of image in edge patches using the same regularization parameter, which causes the low accuracy of denoising output and suffers from halo artifacts.

To address the above problems, a large number of improved methods were proposed, the representatives of which mainly improve parameters of flexibility. For example, an edge-aware weighting was used to penalize the fixed regularization parameter with local variances of all pixels in the 3×3 window, which is to produce a more robust method in [9]. Fei et al. [17] proposed the improved guided image filter in gradient domain, using an explicit first-order edge-aware constraint to distinguish the edge and smooth patch. However, as the information of edge and texture area is disturbed by noise, local variances and first-order gradient in noise image cannot objectively represent change information. The edge-aware weighting factor using local variances or first-order gradient in noise image

is inaccurate. Therefore, it is sensible that we seek a method be efficient in precision edge detection and noise suppression by adaptive weighting regularization parameter.

WGIF is introduced by incorporating a monogenic phase congruency weighting for edge-awareness into an existing guided image filter (GIF) to avoid halo artifacts for image denoising in this paper. The proposed method takes edge-aware weighting by monogenic phase congruency that describes the information of edge and texture into consideration. The proposed filter has also a linear computational cost which is the same as that of the GIF [4].

2. Related Work on Guided Image Filter. The guided image filter in [4] uses a linear transform of the guidance image to preserve preferably edge independent of the filter radius and the range of gray value, and it outperforms the bilateral filter [8]. Under the guidance of different guided images, GIF is widely applied to the field of image process and computer vision, such as enhancing image sharpness without noise amplification, HDR compression, image matting/feathering, dehazing and image fusion.

The guided filter is a general linear translation-variant filter. It is assumed that the output image is a linear transform of a guidance image and a filtering input image. The filtering output f'_i at a pixel i is given as follows:

$$f'_i = \sum_j W_{ij}(G) f_j \quad (1)$$

where f is the filtering input image, G is a guidance image independent of the filtering input image, f'_i is the output image and the filter kernel $W_{ij}(G)$ is a function of the guide image G , but is independent of f . Note that W_{ij} are normalized weights, that is, $\sum_j W_{ij}(G) = 1$.

It is assumed that \bar{Z} is a linear transform of G_k in a window w_i centered at the pixel i . A linear transform \bar{Z} of G in the window w_i is expressed by

$$\bar{Z}(i) = a_i G_k + b_i, \quad \forall k \in w_i \quad (2)$$

where a_i and b_i are two constants in the window w_i , linear coefficients (a_i, b_i) , and w_i is a square window centered at the pixel i of a radius r .

To obtain two coefficients a_i and b_i , it is a solution that minimizes the following cost function $E(a_i, b_i)$ in the window w_i using the linear ridge regression model.

$$E(a_i, b_i) = \sum_{i=1}^N [a_i G_k + b_i - f_i]^2 + \lambda a_i^2 \quad (3)$$

Here, N is the total number of pixels in w_i , and λ is a regularization parameter.

The solution of Equation (3) is given by

$$\begin{cases} a_i = \frac{\frac{1}{N} \sum_{i=1}^N f_i G_i - \bar{f}_k \mu_k}{\sigma_k^2 + \lambda} \\ b_i = \bar{f}_i - a_i \mu_k \end{cases} \quad (4)$$

where, μ_k and σ_k are the mean and variance of G in w_i , and \bar{f}_k is the mean of f_i in the window w_i . Finally, Equation (2) with the average coefficients of all windows overlapping method is modified by

$$\bar{Z}(i) = \bar{a}_i G_i + \bar{b}_i \quad (5)$$

where \bar{a}_i and \bar{b}_i are the average coefficients of all windows overlapping i . For the same reason, it was proved that the GIF is also a weighted averaging filter in [4], and the

weighting kernel function W_{ij} can be explicitly written as

$$W_{ij}(G) = \frac{1}{|w|^2} \sum_{k:(i,j) \in w_k} \left(1 + \frac{(G_i - u_k)(G_j - u_k)}{\sigma_k^2 + \lambda} \right) \quad (6)$$

where $|w|$ is the total number of pixels in a window w_k , λ is a global smoothing parameter, and u_k and σ^2 are the mean and variance of G in w_k .

It is well-known that the guided filter kernel weights can recognize flexibly underlying geometric structures in accordance with the performance of the guide image. Unfortunately, although the GIF has numerous advantages of computer vision and graphics applications, the fixed regularization global smoothing parameter λ cannot adapt to the grey scale difference between flat and edge patches. Specifically, it has poor performance in the low SNR images for image denoising.

To overcome the flaw of the GIF parameters and obtain the excellent result, integrating the shift-variant technique and a Laplacian of Gaussian (LOG) filter response output for pixel classification into the guided filter results to avoid halo artifacts or noise amplification was proposed in [12].

In [4], regularization parameter λ is a constant, so halo artifacts near edge are caused without distinguishing the image structure difference. To solve this problem, regularization parameter of the improved guided image filtering in [9] is defined by another function that is an edge-aware weighting. Regularization parameter $\lambda(i)$ is defined by a weighted factor using local variances of all pixels in the 3×3 window, which is expressed by

$$\lambda(i) = \frac{\lambda}{N} \sum_{i'=1}^N \frac{\sigma_{G,1}^2(i) + \gamma_\sigma}{\sigma_{G,1}^2(i') + \gamma_\sigma} \quad (7)$$

where $\sigma_{G,1}(i)$ is local variance of a 3×3 square window centered at a pixel i of the guidance image, γ_σ is a small constant and its value is selected as $(0.001 \times L)^2$ while L is the dynamic range of the input image. $\lambda(i)$ in Equation (7) can preferably reflect the change of the image detail. Clearly, large weights are assigned to pixels at edges but small weights of those pixels in flat areas are close to 0 using the weight of Equation (7). The weighting function in [9] conforms to one feature of human visual system that the pixels of sharp edges are usually more significant than those in flat areas. The method in [9] can be applied to reducing halo artifacts. However, the local variance linear model cannot represent exactly the image near some edges. To be precise, the more accurate the edges are detected, the better fine details are enhanced by the proposed weighting. However, edge-preserving methods using the local variance cannot preserve edges preferably in some cases in [9].

Recently, a gradient domain GIF was proposed by an edge-aware weighting defining variable window to measure the importance of some pixels with respect to the whole guidance image in [17]. Through the reasonable analysis of window size of the filter, the proposed filter handles images with better visual appearance than the existing guided filter based algorithms, especially around edges. However, the definition of window size of the filter for different images is inextricability.

3. AWGIF Using Monogenic Phase Congruency.

3.1. Monogenic phase congruency. Phase congruency (PC) is a perceptually significant image feature detection method and reflects the behavior of the image in the frequency domain. The phases in the frequency domain have maximal congruency at the edges, which corresponds to the human-perceived edges in an image where there are sharp changes between light and dark.

PC in [15] at some location x over orientation θ and scale s can be expressed as

$$PC_1(x) = \frac{\sum_{\theta} [E_{\theta}(x) - T_{\theta}]}{\sum_{\theta} \sum_s A_{\theta s}(x) + \varepsilon} \tag{8}$$

where $E(x)$ is the local energy and is expressed as $\sqrt{(\sum_s f(x) * M_s^e)^2 + (\sum_s f(x) * M_s^o)^2}$, M_s^e and M_s^o are the even- and odd-symmetric filters on scale s respectively, $A_s(x)$ is the local amplitude, ε is a small positive constant and $[\]$ denotes that the enclosed quantity is not permitted to be negative, T_{θ} compensates for the influence of noise, and its value can be set in terms of estimating empirically or computation through the below method.

The monogenic signal in [16] is considered to be a multi-dimensional extension of Riesz transform. The monogenic signal \mathbf{f}_m of an image $f(x)$ is defined by

$$\mathbf{f}_m(x) = \{f(x), R_{x_1} * f(x), R_{x_2} * f(x)\} \tag{9}$$

The local amplitude (energy), local orientation and the local phase of $f(x)$ over scale s can be expressed by

$$\begin{cases} \mathbf{A}_s(x) = \sqrt{f_s^2(x) + (R_{x_1} * f_s(x))^2 + (R_{x_2} * f_s(x))^2} \\ \varphi_s(x) = -\text{sign}(R_{x_1} * f_s(x)) \text{atan2}(f_s(x), R) \\ \theta_s(x) = \text{atan}\left(\frac{R_{x_2} * f_s(x)}{R_{x_1} * f_s(x)}\right) \end{cases} \tag{10}$$

where $R = \sqrt{(R_{x_1} * f_s(x))^2 + (R_{x_2} * f_s(x))^2}$.

A novel measure of phase congruency that combines with the monogenic signal, which is called monogenic phase congruency was proposed in [11]. This measure approximated the local maximum of amplitude and phase deviation.

Monogenic phase congruency (MPC) can be expressed as

$$MPC(x) = \frac{1}{1 + \exp(\gamma(s - c(x)))} \left[1 - \xi \times \text{acos} \left(\frac{\sqrt{fs^2 + fr_{x_1}^2 + fr_{x_2}^2}}{\sum_{s=1}^N A_s(x)} \right) \right] \frac{[\sqrt{fs^2 + fr_{x_1}^2 + fr_{x_2}^2} - T]}{\sum_{s=1}^N A_s(x) + \varepsilon} \tag{11}$$

where $fs = \sum_s f_s(x)$, $fr_{x_1} = \sum_s (R_{x_1} * f(x))$, $fr_{x_2} = \sum_s (R_{x_2} * f(x))$, γ is a gain factor for the sharpness of the cutoff, s is the cut-off value of filter response spread, and $c(x)$ is a fractional measure of spread. The value of $c(x)$ is obtained by taking the sum of the amplitudes of the responses and dividing by the highest individual response, namely $c(x) = A'(x)/(N * (A_{\max}(x) + \varepsilon))$, N is the total number of scales, and ξ is a gain factor approximately from 1 to 2. T compensates for the influence of noise, and is set a fixed threshold according to empirical estimation.

MPC is speedy and possesses much more reduced memory requirements than the other phase congruency model. Using T for compensating the influence of noise, the MPC response is not sensitive to noise.

3.2. A new edge-aware weighting. Instead of local variance, a new edge-aware weighting using monogenic phase congruency based edge detection methods is proposed. The proposed edge-aware weighting $\Gamma'_G(i)$ is defined by using monogenic phase congruency of

3×3 windows of all pixels as follows:

$$\Gamma'_G(i) = \frac{1}{N} \sum_{i'=1}^N \frac{|MPC(i)| + \gamma'(i)}{|MPC(i')| + \gamma'(i)} \quad (12)$$

where $MPC(i)$ is the value of monogenic phase congruency at the center pixel i , i' is the index of windows of all pixels, γ' is a small constant, and $|\cdot|$ is the expression of absolute values.

Therefore, the filter in Equation (6) is modified by

$$W'_{ij}(G) = \frac{1}{|w|^2} \sum_{k:(i,j) \in w_k} \left(1 + \frac{(G_i - u_k)(G_j - u_k)}{\sigma_k^2 + \lambda/\Gamma_G(i)} \right) \quad (13)$$

After a lot of experiments and tests, it is found that the algorithm is more robust by setting the value γ' using one tenth of the maximum value of $MPC(i)$. At the edge pixels, the values of $MPC(i)$ are large, so the values of $\Gamma'_G(i)$ for the edge pixels are greater than 1 and the values of $W'_{ij}(G)$ are larger than the mean. In that way, the weight assigned to pixel i is large. The results reflect the significance of edge pixels in GIF method, which is consistent with human vision. Whereas, at the flat pixels, the absolute value of $MPC(i)$ becomes small, the values of $\Gamma'_G(i)$ for the flat region pixels are smaller than 1, and even, is close to 0. Accordingly, $W'_{ij}(G)$ is far lower than the mean. As MPC is an approximation method, the time complexity of $\Gamma'_G(i)$ is $O(N)$ for an image with N pixels. The computational cost of $\Gamma'_G(i)$ is in keeping with the calculation of weight $W'_{ij}(G)$. The time complexity of the proposed algorithms is comparable to that of the GIF based algorithms.

According to [4], the filter kernel of AWGIF for image denoising can be shortened as

$$\hat{f}_i = \sum_{j \in w_i} W'_{ij}(G) f_j \quad (14)$$

where \hat{f}_i is the image of removed noise and f_j is the original image pixel in local windows. In principle, the weighting function of AWGIF is similar to the range domain of bilateral filter (BF), as each of them includes the intensity values of the centre pixel i , local neighbours j and a smoothing parameter in the computation process. However, the performance of BF was not as good as that of AWGIF or GIF.

4. Experimental Results and Analysis. In this section, in order to test and compare the performance of our proposed algorithm with other algorithms in the literature, we conduct experiments on ten images of 512×512 pixels from [18] that are widely available such as Pepper, Lena, and House. The noise we use is normal, with standard deviation $\sigma = 10, 20, 30, 40$ and 50 .

4.1. Image-quality evaluation. For the comparison, we used both qualitative and quantitative evaluations to compare, our proposed AWGIF method with other methods. Quantitative evaluations were performed using structural similarity (SSIM) [19] and peak signal-to-noise ratio (PSNR) for full-reference cases in which original high-quality images on large benchmark datasets are available.

Our proposed WGIF was compared with the other five different filtering methods in experiments: the non-local means algorithm (NLM) [1], the original GIF [4], BM3D [5], bilateral filtering (BF) [8], and gradient-domain GIF (GDGIF) [17]. GDGIF is representative of the improved version of GIF from [9], [12] and [17], which gives excellent performance. All algorithms in the experiments were implemented using MATLAB 2010b software, and all the simulations were carried out on an Intel Core 2 Duo T5850 processor with a frequency of 2.16 GHz and 4 GB of DDRII memory running the Windows 7 operating system.

4.2. Results and analysis. The performance of different algorithms were measured quantitatively using PSNR and SSIM. Figures 1 and 2 listed the denoising performance of the different methods for comparison.

First, the original GIF, our proposed GIF, and GDGIF produced outputs of reasonable quality for images with low noise levels from PSNR and SSIM indexes. However, when the noise level increased, the performance of both the original GIF and GDGIF deteriorated drastically. GDGIF performed better than the original GIF because of its better edge-preserving capability. Our proposed GIF did not suffer from noise amplification, and its performance was better than that of the original GIF and GDGIF when the noise levels increased. Our proposed GIF outputs were comparable to those obtained using BF, BM3D and superior to those obtained using any of the other algorithms. Although GDGIF produced images with slightly higher PSNR indexes than our proposed GIF did, our proposed GIF outperformed GDGIF in terms of SSIM indexes. We will discuss these characteristics in more detail from the perspective of execution time.

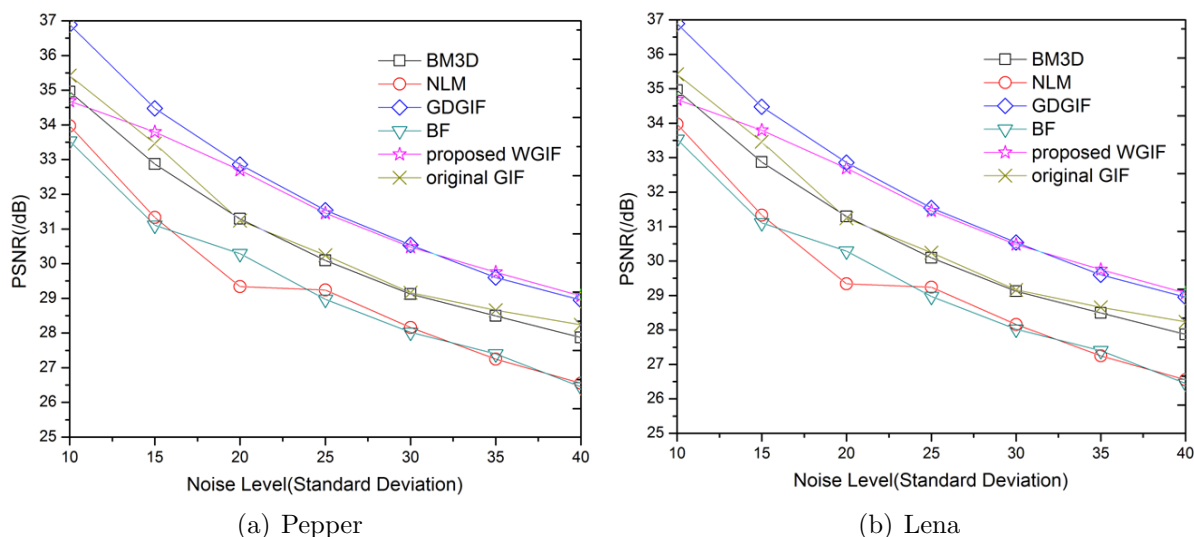


FIGURE 1. Comparison of the average PSNR indexes for the various denoising filtering algorithms

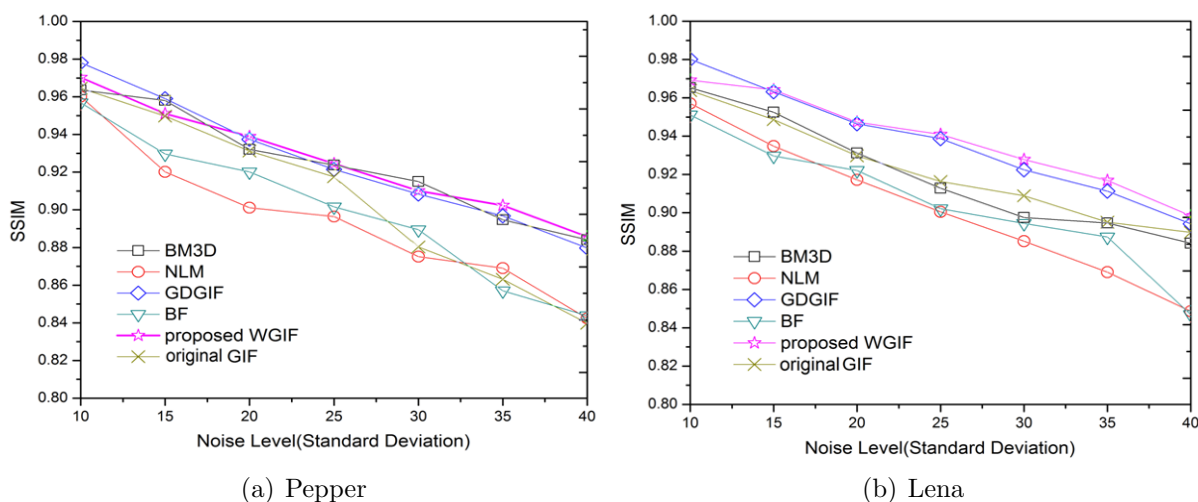


FIGURE 2. Comparison of the average SSIM indexes for the various denoising filtering algorithms

TABLE 1. Comparison of denoising execution time (second)

Algorithm	Size of image and execution time (s)			
	128×128	256×256	512×512	1024×768
NLM	8.59	19.34	39.85	146.36
GDGIF	0.64	1.49	3.42	8.67
Proposed GIF	0.83	1.13	3.01	6.15
BF	0.54	1.69	4.98	10.68

Then, we compare execution times. Comparison of the computation time of our proposed GIF, GDGIF, the NLM algorithm, and BF is shown in Table 1 using three images, each of different size. The table shows that the processing time of our proposed GIF is very low. This is due to the measure of phase congruency based on the monogenic signal and the reduction of orientation and the noise threshold calculation, and the avoidance of dot and cross products. The execution time for phase congruency of our proposed GIF is lower than that of GDGIF for edge detection. BF is fast; however, as the image size increases, the execution time of BF is significantly longer than GIF.

5. Conclusions. The novel weighted guided image filter based on monogenic signal theory is introduced in this paper. Compared to the existing state-of-the-art approaches, the proposed method exhibited improved performance in terms of PSNR and SSIM. The method also demonstrated better generalization performance and lower execution time than its nearest competitors. One more interesting problem is on the extension of the proposed filter so as to extract fine details using multiple images simultaneously. It will be studied in our future research.

Acknowledgment. This work is partially supported by the Doctoral Development Foundation of Panzhihua University and Scientific Foundation of Department of Education of Sichuan Province under grant No. 15ZB0425. The authors also gratefully acknowledge the helpful comments and suggestions of the reviewers, which have improved the presentation.

REFERENCES

- [1] A. Buades, B. Coll and J. M. Morel, A review of image denoising algorithms, with a new one, *Multiscale Modeling & Simulation*, vol.4, no.2, pp.490-530, 2005.
- [2] M. Elad and M. Aharon, Image denoising via sparse and redundant representations over learned dictionaries, *IEEE Trans. Image Processing*, vol.15, no.12, pp.3736-3745, 2006.
- [3] J. Orchard, M. Ebrahimi and A. Wong, Efficient nonlocal-means denoising using the SVD, *Proc. of IEEE International Conference on Image Processing*, San Diego, CA, pp.1732-1735, 2008.
- [4] K. He, J. Sun and X. Tang, Guided image filtering, *IEEE Trans. Pattern Analysis and Machine Intelligence*, vol.35, no.6, pp.1397-1409, 2013.
- [5] K. Dabov, A. Foi, V. Katkovnik et al., Image denoising by sparse 3-D transform-domain collaborative filtering, *IEEE Trans. Image Processing*, vol.16, no.8, pp.2080-2095, 2007.
- [6] S. Li, X. Kang and J. Hu, Image fusion with guided filtering, *IEEE Trans. Image Processing*, vol.22, no.7, pp.2864-2875, 2013.
- [7] K. He, J. Sun and X. Tang, Single image haze removal using dark channel prior, *IEEE Trans. Pattern Analysis and Machine Intelligence*, vol.33, no.12, pp.2341-2353, 2011.
- [8] C. Tomasi and R. Manduchi, Bilateral filtering for gray and color images, *Proc. of the 1998 IEEE International Conference on Computer Vision*, Bombay, India, pp.839-846, 1998.
- [9] Z. Li, J. Zheng, Z. Zhu et al., Weighted guided image filtering, *IEEE Trans. Image Processing*, vol.24, no.1, pp.120-129, 2015.
- [10] D. V. D. Ville and M. Kocher, SURE-based non-local means, *IEEE Signal Processing Letters*, vol.16, no.11, pp.973-976, 2009.
- [11] X. G. Luo, Monogenic signal theory based feature similarity index for image quality assessment, *AEU – International Journal of Electronics and Communications*, vol.69, no.1, pp.75-81, 2015.

- [12] C. C. Pham and J. W. Jeon, Efficient image sharpening and denoising using adaptive guided image filtering, *IET Image Processing*, vol.9, no.1, pp.71-79, 2014.
- [13] A. Hosni, M. Bleyer, C. Rhemann et al., REal-time local stereo matching using guided image filtering, *IEEE International Conference on Multimedia & Expo*, pp.1-6, 2011.
- [14] P. Bauszat, M. Eisemann and M. Magnor, Guided image filtering for interactive high-quality global illumination, *Computer Graphics Forum*, vol.30, no.4, pp.1361-1368, 2011.
- [15] M. C. Morrone and R. A. Owens, Feature detection from local energy, *Pattern Recognition Letters*, vol.6, no.5, pp.303-313, 1987.
- [16] M. Felsberg and G. Sommer, The monogenic signal, *IEEE Trans. Signal Processing*, vol.49, no.12, pp.3136-3144, 2001.
- [17] K. Fei, W. Chen, C. Wen et al., Gradient domain guided image filtering, *IEEE Trans. Image Processing*, vol.24, no.11, pp.4528-4539, 2015.
- [18] Y. Q. Zhang, Y. Ding, J. Liu et al., Guided image filtering using signal subspace projection, *IET Image Processing*, vol.7, no.3, pp.270-279, 2013.
- [19] Z. Wang, A.-C. Bovik, H.-R. Sheikh and E.-P. Simoncelli, Image quality assessment: Form error visibility to structural similarity, *IEEE Trans. Image Processing*, vol.13, no.4, pp.600-612, 2004.
- [20] N. D. Narvekar and L. J. Karam, A no-reference image blur metric based on the cumulative probability of blur detection (CPBD), *IEEE Trans. Image Processing*, vol.20, no.9, pp.2678-2683, 2011.
- [21] K. Ito and K. Xiong, Gaussian filters for nonlinear filtering problems, *IEEE Trans. Automatic Control*, vol.45, no.5, pp.910-927, 2000.